Effects of transparent MPTMS/Ag/MoO_3 structure as anode on the performance of green organic light-emitting diodes*

HU Jun-tao (胡俊涛)[1,2]**, **DENG Ya-fei** (邓亚飞)[1,2,3], **MEI Wen-juan** (梅文娟)[1,2], and **YANG Jing-song** (杨劲松)[1,2]

1. *National Engineering Laboratory for Special Display Technology, Key Laboratory of Special Display Technology, Ministry of Education of China, Province and Ministry State Key Laboratory of Advanced Display Technology, Hefei 230009, China*
2. *Academy of Photoelectric Technology, Hefei University of Technology, Hefei 230009, China*
3. *School of Instrument Science and Opto-electronics Engineering, Hefei University of Technology, Hefei 230009, China*

(Received 3 July 2015)

©Tianjin University of Technology and Springer-Verlag Berlin Heidelberg 2015

A transparent 3-mercaptopropyl trimethoxysilane (MPTMS)/Ag/MoO_3 composite anode is introduced to fabricate green organic light-emitting diodes (OLEDs). Effects of the composite anode on brightness and operating voltage of OLEDs are researched. By optimizing the thickness of each layer of the MPTMS/Ag/MoO_3 structure, the transmittance of MPTMS/Ag (8 nm)/MoO_3 (30 nm) reaches over 75% at about 520 nm. The sheet resistance is 3.78 Ω/□, corresponding to this MPTMS/Ag (8 nm)/MoO_3 (30 nm) structure. For the OLEDs with the optimized anode, the maximum electroluminescence (EL) current efficiency reaches 4.5 cd/A, and the maximum brightness is 37 036 cd/m^2. Moreover, the OLEDs with the optimized anode exhibit a very low operating voltage (2.6 V) for obtaining brightness of 100 cd/m^2. We consider that the improved device performance is mainly attributed to the enhanced hole injection resulting from the reduced hole injection barrier height. Our results indicate that employing the MPTMS/Ag/MoO_3 as a composite anode can be a simple and promising technique in the fabrication of low-operating voltage and high-brightness OLEDs.

Document code: A **Article ID:** 1673-1905(2015)05-0333-5
DOI 10.1007/s11801-015-5125-8

In organic light-emitting diodes (OLEDs), tin-doped indium oxide (ITO), owing to its high optical transparency in the visible spectrum and commercial availability, has been exclusively used as a preferred anode. However, ITO has some disadvantages, such as high cost, relatively low work function, limited use for flexible substrates and degradation of device performance over time due to indium diffusion[1,2]. So far, many materials have been used to replace ITO as electrodes, such as Cu/graphene[3], indium zinc oxide (IZO) protected silver film[4], poly(3,4-ethylenedioxythiophene) (PEDOT) film[5] and carbon nanotube[6].

On the other hand, metals, such as Ag, Al, Au and Cu, have been reported as anodes of OLEDs[7-9]. Among these metals, Ag is regarded as one of the best choices for the electrode of OLEDs, because it has the lowest electrical resistivity (~1.6 μΩ·cm for bulk material at 300 K)[10]. However, very thin metal films deposited on glass or SiO_2 substrates are discontinuous because they grow in Volmer-Weber mode. 3-mercaptopropyl trimethoxysilane (MPTMS) is known to bind to coinage metal surfaces via a strong covalent linkage by forming well-ordered self-assembled monolayers (SAMs) on SiO_2[11]. A thinner continuous Ag film can be prepared on a thermal oxide of Si or a glass substrate with an MPTMS interlayer due to the strong interaction between Ag atoms and the mercapto moiety of MPTMS, and Ag thin films grown on MPTMS interlayer are flatter and have a lower resistivity than those grown without an interlayer[12]. However, Ag is generally not considered as an ideal hole injection anode for OLEDs due to its rather low work function (~4.7 eV), which does not match well with the ionization potentials of organic materials commonly used in OLEDs[10]. Besides, MoO_3 as an an-

* This work has been supported by the National Natural Science Foundation of China (No.21174036), the National High Technology Research and Development Program of China (863 Program) (No.2012AA011901), and the National Basic Research Program of China (973 Program) (No.2012CB723406).

** E-mail: jthu@hfut.edu.cn

ode modifier or dopant for the hole injection layer significantly reduces the operational voltage and greatly improves the efficiency and lifetime of OLEDs[13,14]. And the variation of the thickness of MoO_3 layers can strongly modify the optical properties of the multilayer anodes[15]. Little consideration has been given to using the MoO_3/Ag/MPTMS as an anode of green OLEDs.

In this paper, we prepare Ag and MoO_3 thin films with various thicknesses on glass substrates with an MPTMS interlayer, and their electrical and optical properties are investigated. Then, we use the optimized Ag and MoO_3 with an MPTMS interlayer as the anode in OLEDs with the same structure. The properties of the device with an MoO_3/Ag/MPTMS anode are compared with those using an ITO anode.

The ITO coated glass samples with a sheet resistance of 15 Ω/□ were purchased from Luminescence Technology Corp. 3-mercaptopropyl trimethoxysilane (MPTMS) with purity of 95% is used as an SAM material from sigma-aldrich. N,N′-Di(naphthalene-1-yl)-N,N′-diphenyl-benzidine (NPB) with purity of 99% is used as a hole-transport material, and tris-(8-hydroxyquinoline) aluminium (Alq_3) with purity of 99% is used as an emission material from Luminescence Technology Corp. The electron-transport material of LiF (99% purity), and the hole injection material of MoO_3 (99% purity) were purchased from Luminescence Technology Corp. Ag (99.99% purity) was obtained from sigma-aldrich.

All of the thin films except the SAM were fabricated using a deposition chamber (AMOD, Angstrom). The layer thicknesses of the deposited materials were monitored using an oscillating quartz thickness monitor. The current density-voltage (*J-V*) characteristics of the OLEDs were measured using a Keithley 2400 source measure unit. The electroluminescence (EL) spectrum and luminance were recorded with Spectroradiometer SR-UL1R (Topcon Co.). The electrical resistance was measured at room temperature by the four-point probe method. The optical transmittance was measured using an ultraviolet/visible (UV/vis) spectrophotometer.

The patterned ITO glass and the glass substrates were first ultrasonic cleaned successively in acetone, ethanol and deionized water. The moisture was thoroughly removed by nitrogen (N_2) gas flow. To ensure complete removal of all the remaining water, the patterned ITO glass and the glass substrates were heated on a hot plate for 10 min at 100 °C. For hydrophilic treatment of the patterned ITO glass, it was cleaned for 10 min in a UV ozone (UVO) cleaner. The cleaned ITO glass was used immediately to prepare the OLED devices.

On the other hand, after drying by N_2 stream, the glass substrates were then treated in a UVO cleaner for 30 min to increase the surface composition of hydroxyl groups. The cleaned glass substrates were immersed into the mixed solution immediately for forming SAM layers on surfaces. MPTMS and toluene were mixed with bulk ratio of 1:40. After 6 h reaction at room temperature, the substrates were rinsed by toluene to remove the residual silane and finally dried in an N_2 stream. The SAM-modified glass substrates were used immediately to prepare the OLED devices.

The cleaned ITO glass and glass substrates were loaded immediately into a deposition chamber housed in an N_2 glove box. Ag films were deposited on glass substrates with an MPTMS interlayer by vacuum evaporation with pressure below 2.7×10^{-4} Pa using an Ag wire as the evaporation source. The effect of Ag layer thickness on optical and electrical performance is studied with thicknesses of 4 nm, 5.6 nm, 8 nm and 10 nm. After the deposition of Ag film, an MoO_3 film was deposited using vacuum evaporation with pressure below 2.7×10^{-4} Pa. The effect of MoO_3 layer thickness on optical and electrical performance is studied with thicknesses of 10 nm, 20 nm, 30 nm, 40 nm, 50 nm and 60 nm.

High purity source materials of NPB, Alq_3, LiF and Al were successively evaporated on MoO_3/Ag/MPTMS anode prepared at pressure below 2.7×10^{-4} Pa. Three OLED structures were fabricated as glass/ITO/NPB (40 nm)/Alq_3 (60 nm)/LiF (1 nm)/Al (150 nm), glass/ITO/MoO_3 (10 nm)/NPB (40 nm)/Alq_3 (60 nm)/LiF (1 nm)/Al (150 nm) and glass/MPTMS/Ag/MoO_3/NPB (40 nm)/Alq_3 (60 nm)/LiF (1 nm)/Al (150 nm) as shown in Fig.1.

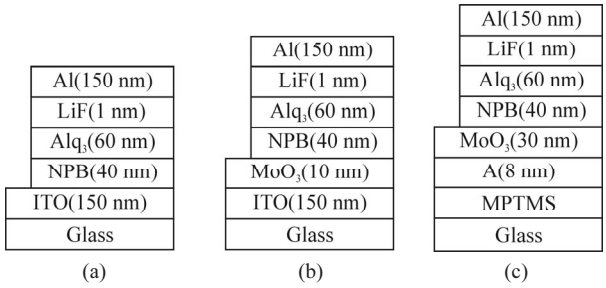

Fig.1 OLED structures with (a) ITO, (b) ITO/MoO_3 and (c) MPTMS/Ag/MoO_3 as anodes

Fig.2 shows the sheet resistances (R_s) of MPTMS/Ag films with various thicknesses. It can be seen that the sheet resistance decreases rapidly from 62 Ω/□ to 10.7 Ω/□ when the Ag layer thickness changes from 4 nm to 5.6 nm, and decreases slowly with the Ag thickness when it is over 5.6 nm. When the Ag thickness is 10 nm, the sheet resistance is 2.74 Ω/□. The sheet resistance of the MPTMS/Ag films with 8 nm-thick Ag film in this study (3.78 Ω/□) is much lower than that of the ITO film (15 Ω/□). Changes in sheet resistance between MPTMS/Ag films with Ag layer thicknesses of 4 nm and 5.6 nm can be attributed to the transition of Ag atoms from distinct islands to continuous film[16].

Fig.3 shows the optical transmission spectra of glass/MPTMS and glass/MPTMS/Ag structures with Ag film thicknesses of 4 nm, 5.6 nm, 8 nm and 10 nm. We can see that the transmittance of the MPTMS/Ag multilayer depends on the thickness of Ag layer. Although the transmittances of these samples cannot be directly compared, the transmittances at the peak emission wavelength of Alq_3 about 520 nm for 4 nm, 5.6 nm and

8 nm-thick Ag films are almost the same. A higher loss in transparency is observed for the Ag layer with thickness of 10 nm. Finally, the thickness of 8 nm is selected for the Ag layer to obtain the optimum electrode.

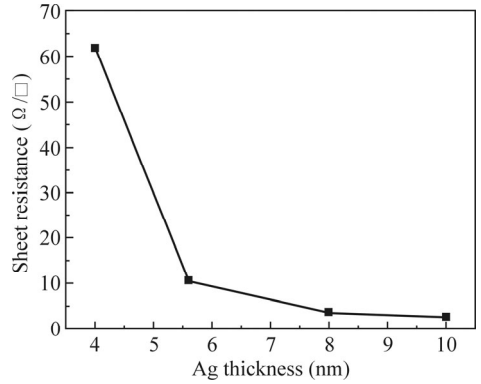

Fig.2 Sheet resistance of MPTMS/Ag film on glass substrate as a function of Ag film thickness

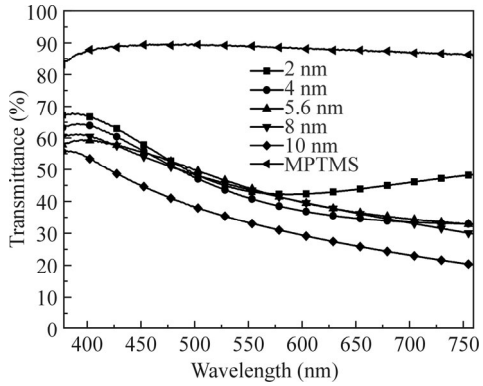

Fig.3 Optical transmission spectra of glass/MPTMS and glass/MPTMS/Ag structures with Ag film thicknesses of 4 nm, 5.6 nm, 8 nm and 10 nm, respectively

Following the optimization of Ag film thickness, the MoO_3 layer is studied by investigating the influence of its thickness on the whole structure transmittance and conductivity. Fig.4 shows the transmittance spectra measured from electrodes with structure of glass/MPTMS/Ag (8 nm)/MoO_3 (*X* nm) with *X* of 10, 20, 30, 40, 50 and 60. It can be seen that the transmittance of the structure at about 520 nm increases with the MoO_3 film thickness up to 30 nm, and decreases when the thickness is beyond 30 nm, while the conductivity only increases slightly. The maximum transmittance reaches over 75% for the case of MPTMS/Ag (8 nm)/MoO_3 (30 nm) at 520 nm. When the MoO_3 thickness increases from 10 nm up to 60 nm, a red shift effect of the transmission spectrum is also observed. Finally, the thickness of 30 nm is selected for the MoO_3 layer to obtain the optimum electrode.

The OLED devices shown in Fig.1 were fabricated. Fig.5 shows the current density-voltage, voltage-luminance and current density-current efficiency characteristics of the devices based on the bare ITO, ITO/MoO_3 (10 nm) and the MPTMS/Ag (8 nm)/MoO_3 (30 nm) anodes, respectively. As expected, the highest current density is observed in Fig.5(a) for MPTMS/Ag/MoO_3 anode. The voltage at a current density of 200 mA/cm^2 is about 9.8 V for the device with bare ITO anode, the voltage is at about 7.6 V for the device with ITO/MoO_3 anode, and it is reduced to about 6.2 V for the device with MPTMS/Ag/MoO_3 anode. The results indicate that the improvement of the current density is related to the improved hole injection by incorporating MPTMS modified Ag and MoO_3 layers as anode into the device architecture. Further proof for the improvement of hole injection by MPTMS/Ag/MoO_3 anode can be seen in the luminance-voltage characteristics of the devices shown in Fig.5(b). The improvement of the luminance performance is very significant. The luminance is higher through the whole voltage range compared with those of the other two devices, indicating a lower driving voltage for the device using the MPTMS/Ag/MoO_3 as anode. The operating voltage is as low as 2.6 V for obtaining brightness of 100 cd/m^2, and the maximum brightness is 37 036 cd/m^2 for the device using the MPTMS/Ag/MoO_3 as anode. Schematic diagrams of energy levels for devices with bare ITO, ITO/MoO_3 and MPTMS/Ag/MoO_3 as anodes are shown in Fig.6. The improved performance of the device with MPTMS/Ag/MoO_3 anode can be explained as follows. We can see that MPTMS/Ag film in emitting device exhibits a higher work function (−5.1 eV) than ITO (−4.7 eV). Therefore, the hole injection barrier is greatly decreased. The improvement of current density and luminance observed in the device with MPTMS/Ag/ MoO_3 as anode is attributed to the matching of highest occupied molecular oribital (HOMO) levels for hole injection from the interfacial layer into the NPB layer. It is well known that MoO_3 is a wide-gap material with a band gap of 3.1 eV and a super hole injection material for anode, and the hole injection barrier from the anode to the hole transport layer (HTL) is lowered. The MoO_3 layer acts as a bridge for efficient hole injection[17,18].

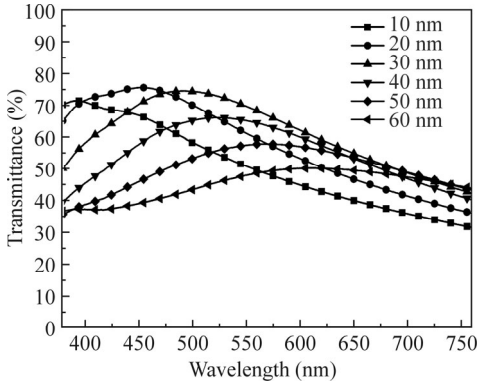

Fig.4 Optical transmittance spectra of glass/MPTMS/Ag (8 nm)/MoO_3 (*X* nm) structures with *X* of 10, 20, 30, 40, 50 and 60

Fig.5(c) shows the current efficiency-current density characteristics for the devices. The device using the MPTMS/Ag/MoO_3 as anode exhibits a little higher current efficiency (4.5 cd/A) than the devices using bare ITO (3.7 cd/A) and ITO/MoO_3 (4.0 cd/A) as anodes. It indicates that the good emission properties are obtained despite the lower optical transmittance of the MPTMS/Ag/MoO_3 anode. It is conceivable that the improved hole injection leads to the more balance of the carriers in emitting zone, then increases the current efficiency and decreases the operating voltage.

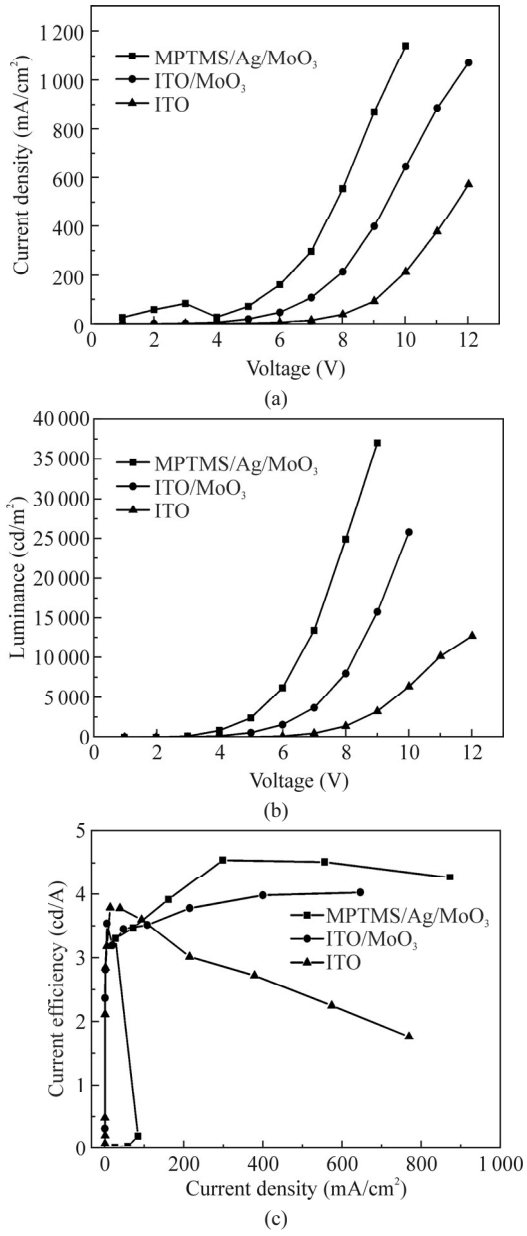

Fig.5 (a) Current density-voltage, (b) luminance-voltage and (c) current efficiency-current density characteristics of the devices fabricated on the bare ITO, ITO/MoO_3 (10 nm) and MPTMS/Ag (8 nm)/MoO_3 (30 nm) anodes

Fig.7 shows the normalized EL spectra of the devices fabricated on the bare ITO, ITO/MoO_3 (10 nm) and the MPTMS/Ag (8 nm)/MoO_3 (30 nm) anodes, respectively. There is a strong F-P effect in the MPTMS/Ag/MoO_3 anode device[19]. Such a cavity effect narrows the emission spectrum. Then, the morphological analysis is carried out for the deposited samples. Fig.8 shows the atomic force microscopy (AFM) images of the MPTMS interlayer on glass substrates with and without 8 nm-thick Ag thin film. It is-clearly observed that Ag grains are grown small in peanut shape, connected with each other on the MPTMS interlayer. The root-mean- square (*RMS*) roughness of Ag film with the MPTMS interlayer is as low as 1 nm. Consequently, we confirm that the Ag film grows flat on a glass substrate with

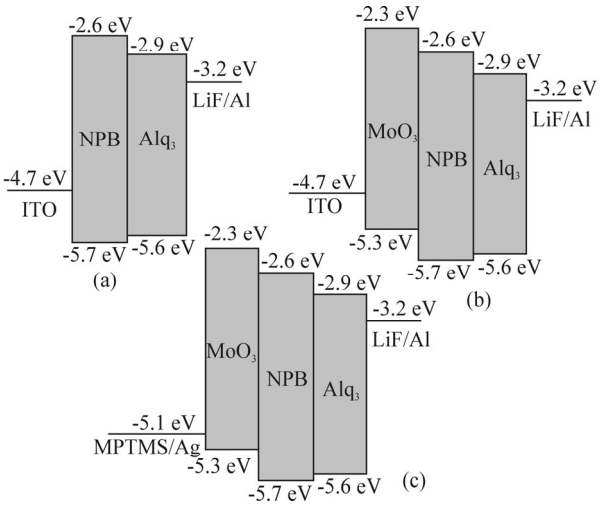

Fig.6 Schematic diagrams of energy level for the green OLEDs with (a) ITO, (b) ITO/MoO_3 and (c) MPTMS/Ag/MoO_3 anodes

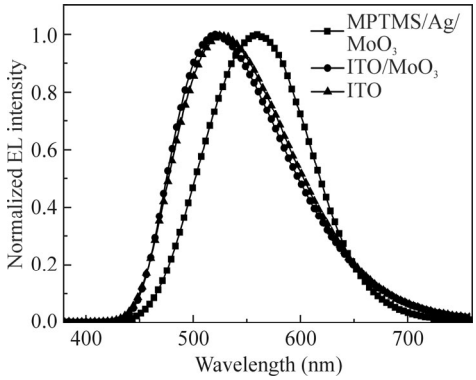

Fig.7 Normalized EL spectra of OLED devices with ITO, ITO/MoO_3 and MPTMS/Ag/MoO_3 anodes, respectively

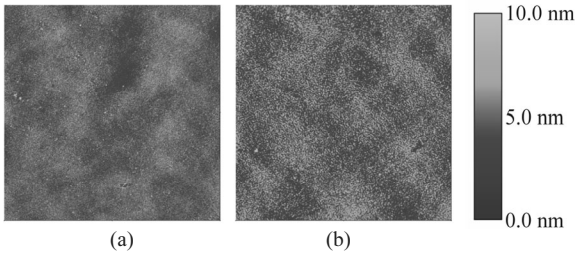

Fig.8 AFM images of the MPTMS interlayer on glass substrates (a) with and (b) without 8 nm-thick Ag thin film (Image size is 5 μm×5 μm.)

the MPTMS interlayer. Undoubtedly, the performance can be further improved after the optimization of OLED structure materials.

In conclusion, we demonstrate the low-voltage and high-brightness green OLEDs with the optimized MPTMS/Ag/MoO_3 anode. Our results show that the optimized MPTMS/Ag/MoO_3 anode not only shows high transmittance at 520 nm, but also considerably enhances the brightness and reduces the operating voltage. The introduction of the MoO_3 layer on Ag layer greatly regulates the transmittance of the MPTMS/Ag/MoO_3 anode and the hole injection barrier from the metal anode to the HTL. Therefore, ITO-free OLED devices can be fabricated by replacing ITO with thin MPTMS/Ag/MoO_3 anode.

References

[1] Darran R Cairns, Richard P. II Witte, Daniel K Sparacin, Suzanne M. Sachsman, David C. Paine, Gregory P. Crawford and R. R. Newton, Applied Physics Letters **76**, 1425 (2000).

[2] S. T. Lee, Z. Q. Gao and L. S. Hung, Applied Physics Letters **75**, 1404 (1999).

[3] Hu Meng, Jianxing Luo, Wei Wang, Zujin Shi, Qiaoli Niu, Lun Dai and Guogang Qin, Advanced Functional Materials **23**, 3324 (2013).

[4] Mingjie Zhao, Jianhua Zou, Yueju Su, Ruixia Xu, Jiawei Pang, Lang Wang, Miao Xu, Hong Tao, Lei Wang and Junbiao Peng, ECS Journal of Solid State Science and Technology **2**, R190 (2013).

[5] Yuxin Li, Xiujie Hu, Shuyun Zhou, Li Yang, Jun Yan, Chenghua Sun and Ping Chen, Journal of Materials Chemistry C **2**, 916 (2014).

[6] LI Xiao-yun, HU Wen-zheng and LIU Guo-rui, Journal of Optoelectronics·Laser **25**, 1855 (2014). (in Chinese)

[7] F. Laurent M. Sam, M. Anas Razali, K. D. G. Imalka Jayawardena, Christopher A. Mills, Lynn J. Rozanski, Michail J. Beliatis and S. Ravi P. Silva, Organic Electronics **15**, 3492 (2014).

[8] H. M. Zhang and Wallace C. H. Choy, Organic Electronics **9**, 964 (2008).

[9] Helena M. Stec and Ross A. Hatton, ACS Applied Materials and Interfaces **4**, 6013 (2012).

[10] Chieh-Wei Chen, Ping-Yuan Hsieh, Huo-Hsien Chiang, Chun-Liang Lin, Han-Ming Wu and Chung-Chih Wu, Applied Physics Letters **83**, 5127 (2003).

[11] Minghui Hu, Suguru Noda, Yoshiko Tsuji, Tatsuya Okubo, Yukio Yamaguchi and Hiroshi Komiyama, Journal of Vacuum Science & Technology A: Vacuum, Surfaces, and Films **20**, 589 (2002).

[12] M. Kawamura, T. Fudei and Y. Abe, Journal of Physics **417**, 012004 (2013).

[13] Zhang Hongmei, Xiao Jianjian, Zeng wenjin and Huang Wei, Displays **35**, 171 (2014).

[14] Yongwon Kwon, Yongnam Kim, Hyunkoo Lee, Changhee Lee and Jeonghun Kwak, Organic Electronics **15**, 1083 (2014).

[15] D.-T. Nguyen, S. Vedraine, L. Cattin, P. Torchio, M. Morsli, F. Flory and J. C. Bernède, Journal of Applied Physics **112**, 063505 (2012).

[16] Terumasa Fudei, Midori Kawamura, Yoshio Abe and Katsutaka Sasaki, Journal of Nanoscience and Nanotechnology **12**, 1188 (2012).

[17] Baolin Tian, Investigation of MoO_3 as an Electron Injection Contact and as a Charge Transport Material in Transparent Organic Light Emitting Devices, Canada: University of Waterloo, 2011.

[18] LIN Hui, YU Jun-sheng and ZHANG Wei, Optoelectronics Letters **8**, 197 (2012).

[19] ZHANG Mai-li, ZHANG Fang-hui, ZHANG Wei and ZHANG Si-lu, Journal of Optoelectronics·Laser **24**, 888 (2013). (in Chinese)